





# The development of cortical functional hierarchy is associated with the molecular organization of prenatal/postnatal periods

Yuxin Zhao <sup>1,2,†</sup>, Meng Wang <sup>1,2,†</sup>, Ke Hu <sup>1,2</sup>, Qi Wang <sup>1,2</sup>, Jing Lou <sup>3</sup>, Lingzhong Fan <sup>1,2,4</sup>, Bing Liu <sup>3,5,\*</sup>

<sup>1</sup>Brainnetome Center and National Laboratory of Pattern Recognition, Institute of Automation, Chinese Academy of Sciences, Beijing 100190, China,

<sup>2</sup>School of Artificial Intelligence, University of Chinese Academy of Sciences, Beijing 100049, China,

<sup>3</sup>State Key Laboratory of Cognitive Neuroscience and Learning, Beijing Normal University, Beijing 100875, China,

<sup>4</sup>CAS Center for Excellence in Brain Science and Intelligence Technology, Institute of Automation, Chinese Academy of Sciences, Beijing 100190, China,

<sup>5</sup>Chinese Institute for Brain Research, Beijing 102206, China

\*Corresponding author: State Key Laboratory of Cognitive Neuroscience and Learning, Beijing Normal University, Beijing 100875, China. Email: bing.liu@bnu.edu.cn

†Yuxin Zhao and Meng Wang contributed equally to the work.

The human cerebral cortex conforms to specific functional hierarchies facilitating information processing and higher-order cognition. Prior studies in adults have unveiled a dominant functional hierarchy spanning from sensorimotor regions to transmodal regions, which is also present in younger cohorts. However, how the functional hierarchy develops and the underlying molecular mechanisms remain to be investigated. Here, we set out to investigate the developmental patterns of the functional hierarchy for preschool children (#scans = 141, age = 2.41–6.90 years) using a parsimonious general linear model and the underlying biological mechanisms by combining the neuroimaging developmental pattern with two separate transcriptomic datasets (i.e. Allen Human Brain Atlas and BrainSpan Atlas). Our results indicated that transmodal regions were further segregated from sensorimotor regions and that such changes were potentially driven by two gene clusters with distinct enrichment profiles, namely prenatal gene cluster and postnatal gene cluster. Additionally, we found similar developmental profiles manifested in subsequent developmental periods by conducting identical analyses on the Human Connectome Projects in Development (#scans = 638, age = 5.58–21.92 years) and Philadelphia Neurodevelopment Cohort datasets (#scans = 795, age = 8–21 years), driven by concordant two gene clusters. Together, these findings illuminate a comprehensive developmental principle of the functional hierarchy and the underpinning molecular factors, and thus may shed light on the potential pathobiology of neurodevelopmental disorders.

**Key words:** cortical development; fMRI; gene expression; postnatal; prenatal.

## Introduction

The human cerebral cortex consists of functionally distinct regions intrinsically organized along multiple large-scale hierarchical axes (hierarchies) that reflect continuous variations of cortical properties and mediate higher-order cognitive functions in response to environmental and physiological stimuli (Burt et al. 2018; Huntenburg et al. 2018; Raut et al. 2020). Importantly, these complex and large-scale functional hierarchies of the adult human cerebral cortex have been well characterized by dimensionality reduction of the functional connectome (Margulies et al. 2016). Notably, the functional hierarchy along the sensorimotor-to-transmodal (S-T) axis (S-T functional hierarchy), corresponding to the intrinsic cortical geometry and paralleling anatomical (Burt et al. 2018) as well as evolutionary hierarchies (Hill et al. 2010; Buckner and Krienen 2013), has received great concern. Anchored by, at one end, sensorimotor cortical regions, and at the other end, transmodal cortical regions (i.e. the default network in humans), the S-T functional hierarchy is assumed to guide the information propagation of sensory inputs and to further facilitate the advanced mental processes in the transmodal cortical regions (Mesulam 2012), as the functional distance from sensory inputs strongly enables the establishment of higher-order cognitive states (Murphy et al. 2018). More interestingly,

the S-T functional hierarchy is gradually believed to be involved in multiple neurocognitive processes (Huntenburg et al. 2018; Sydnor et al. 2021) as well as neurodevelopmental disorders (Hong et al. 2019; Dong, Yao, et al. 2021). In addition, studies have shown that the S-T functional hierarchy undergoes a connectome gradient between the sensorimotor and transmodal regions of the brain during developmental processes of late-childhood to adolescents (Nenning et al. 2020; Xia et al. 2022). The predecessor of S-T functional hierarchy has also been detected in neonates (Larivière et al. 2020), however, how the S-T functional hierarchy matures during early developmental stages remains enigmatic and can be a crucial developmental phase when the atypical neurodevelopmental processes may trigger chronic neurological disorders such as the autism spectrum disorder (ASD).

Studies have demonstrated that the maturation and differentiation processes of the functional organization in the cortex are driven by complex molecular and cellular mechanisms involving heritable genetic factors (Glahn et al. 2010; Silbereis et al. 2016; Bertolero et al. 2019; Reineberg et al. 2020). Twin-based analyses have revealed that the genetic patterning of cortical thickness and surface area is consistent with functionally defined boundaries (Chen et al. 2012, 2013), supporting the genetic determining role in cortical functional organization. Moreover, gene expression

profiles are also concordant with the spatial topography of the cortex (Hawrylycz et al. 2012). Furthermore, functional organization of the cortex mainly depends on the combinatorial proportion of distinct cell types. For example, projection neurons mainly serve as forming long-range cortical circuits, laying structural foundation for the functional connectome (Custo Greig et al. 2013). However, the molecular signatures underlying the macroscale cortical functional hierarchy development remains poorly understood. Therefore, understanding the developmental principles of the cortical functional organization and the underlying molecular mechanisms might be the key to delineating the pathomechanisms of major neurodevelopmental disorders.

Based on the intriguing evidence, we hypothesized that the cortical S-T functional hierarchy might gradually develop from early childhood to adulthood and largely depend on the canonical molecular signatures for the timely segregation of the functional hierarchy. Here, we set out to investigate the developmental pattern of the S-T functional hierarchy in young children (aged 2.41–6.90 years) by applying a parsimonious general linear model (GLM) onto the Calgary Preschool dataset (Reynolds et al. 2020). To accurately elucidate the molecular signatures underlying the S-T functional hierarchy development, we employed the imaging transcriptomic analyses strategy, as in previous studies (Grothe et al. 2018; Morgan et al. 2019; Romero-Garcia et al. 2019; Martins et al. 2021), to dissect the disease, gene ontology (GO), and cell-type enrichment profiles, in reference to the whole-brain transcriptome derived from the Allen Human Brain Atlas (AHBA). A concern may arise for the age mismatch phenomenon between the early childhood neuroimaging dataset (i.e. Calgary Preschool dataset) and the adulthood transcriptome dataset (i.e. AHBA). However, recent evidences have demonstrated that gene expression changes slow markedly after entering into early childhood with the fastest changes before birth, followed by infancy periods (Colantuoni et al. 2011; Kang et al. 2011). Since currently there is no early childhood whole-brain transcriptome dataset available, here, we assume that the adulthood transcriptome dataset may characterize the essentially similar gene expression profile of childhood and adolescents. To further functionally categorize the genes related to the development of the S-T functional hierarchy, we performed cluster analysis of the relevant genes identified based on their temporal expression profiles in the cortex, with respect to the BrainSpan Atlas (<http://www.brainspan.org>), followed by the enrichment analysis for each cluster of genes. Finally, to confirm our hypothesis could also be applied to subsequent developmental stages, we conducted similar analyses using the Human Connectome Projects in Development (HCP-D) (Harms et al. 2018) and Philadelphia Neurodevelopment Cohort (PNC) (Satterthwaite et al. 2014) with subject age ranges of 5.58–21.92 years and 8–21 years, respectively.

## Materials and methods

### Neuroimaging data acquisition

To investigate the developmental pattern of the S-T functional hierarchy, we exploited three independent developmental datasets collectively spanning a large age range. Details of these three datasets are described in the following text:

#### Calgary Preschool dataset

The Calgary Preschool magnetic resonance imaging (MRI) dataset, released by the Developmental Neuroimaging Lab at the University of Calgary, was aimed to characterize typical development during early childhood (Reynolds et al. 2020). Here,  $n = 169$  passive

viewing functional MRI (fMRI) scans were initially drawn from the Calgary Preschool MRI dataset, for which the corresponding T1 images were available. The passive viewing fMRI scans were acquired with a gradient-echo, echo-planar imaging (GE-EPI) sequence ( $3.59 \times 3.59 \times 3.6$  mm<sup>3</sup> resolution, 36 slices, time repetition [TR]/time echo [TE] = 2,000/30 ms), when children were watching a movie of their choice (movie choice was not available). Each child was scanned multiple times at approximately 6-month intervals. Thus, multiple scans were available for each child. Herein,  $n = 141$  scans (age = 2.41–6.90 years, sex = 65F/76M, from  $n = 60$  subjects) remained for further analysis after quality control (QC). See “Data exclusion criteria” for details of QC. For convenience, the passive viewing fMRI scans were referred to throughout the text as resting-state fMRI (rs-fMRI) scans as well.

#### HCP-D dataset

The HCP-D study (Harms et al. 2018) was committed to charting the typical developmental pattern of human brain connectome during childhood and the transition through puberty to young adulthood. Here, all rs-fMRI scans were initially downloaded from the HCP-D release 2.0 dataset. The rs-fMRI scans were acquired with a 2D multiband gradient-recalled echo, EPI sequence ( $2 \times 2 \times 2$  mm<sup>3</sup> resolution, 72 slices, TR/TE = 800/37 ms), with the subjects being awake and fixating at the displayed crosshair. Notably, the downloaded rs-fMRI scans already underwent the HCP minimal preprocessing pipelines (Glasser et al. 2013) and the FMRIB Software Library FIX (Salimi-Khorshidi et al. 2014) denoising procedure. Four scans were available for the older subjects (8–21 years) and 6 scans were available for the younger subjects (5–7 years). The officially concatenated scans for each subject ( $n = 652$  scans) were used in our study. And,  $n = 638$  scans (age = 5.58–21.92 years, sex = 346F/292M) remained for further analysis after QC. See “Data exclusion criteria” for details of QC.

#### PNC dataset

The PNC (Satterthwaite et al. 2014) is a large-scale study funded by the National Institute of Mental Health to characterize the typical development and delineate the abnormal neurodevelopmental mechanisms associated with psychiatric disorders. Here,  $n = 1391$  rs-fMRI scans from the PNC dataset were initially included in our study, for which the corresponding T1 images were available. The rs-fMRI scans were acquired with a single-shot, interleaved multislice, GE-EPI sequence ( $3 \times 3 \times 3$  mm<sup>3</sup> resolution, 46 slices, TR/TE = 3,000/32 ms), with the subjects instructed to stay awake and fixate at the displayed crosshair. The  $n = 795$  scans (age = 8–21 years, sex = 429F/209M) remained for further analysis after QC. See “Data exclusion criteria” for details of QC.

### Rs-fMRI processing

#### Preprocessing

For the Calgary Preschool and PNC datasets, rs-fMRI scans were preprocessed by C-PAC (<https://fcp-indi.github.io/>) for slice-time correction, head motion correction, skull skipping, and intensity normalization, followed by nuisance regression with effects of head motion (including linear/quadratic trends), white matter signals, and cerebrospinal fluid signals as regressors, and the band-pass filtering (0.01–0.1 Hz). The band-passed rs-fMRI scans were then coregistered to a pediatric Montreal Neurological Institute (MNI) template derived from 324 individuals aged 4.5–18.5 years (Fonov et al. 2011). For the HCP-D dataset, all rs-fMRI scans were subjected to the HCP minimal preprocessing pipelines (Glasser et al. 2013) and FIX (Salimi-Khorshidi et al. 2014) denoising

procedure. Additionally, we band-passed (0.01–0.1 Hz) and normalized the concatenated scans for each subject.

### Data exclusion criteria

To mitigate the effects of poor data quality on our results, we screened the above-mentioned neuroimaging datasets according to the following data exclusion criteria:

- (1) Poor medical condition (for PNC dataset only): PNC dataset provided a medical rating score indicating the severity of a patient's medical condition. The score ranged from 0 to 5 (0=no medical problems; 1=minor, no central nervous system impact; 2=moderate; 3=significant; and 4=major). Here, we excluded subjects with a score  $\geq 2$ . The  $n=547$  scans were excluded in this step for the PNC dataset.
- (2) Poor image quality for preprocessing:  $n=3$  scans from the Calgary Preschool dataset were discarded at the image preprocessing step due to poor image quality.
- (3) Large head motion: For the Calgary Preschool and PNC datasets, we selected the mean relative root mean square (RMS) framewise displacement (FD) of a rs-fMRI scan as head motion metric. For the HCP-D dataset, as all the rs-fMRI scans were in the form of the concatenation of multiple scans, we regarded the mean of mean relative RMS FD of the concatenated scans as the overall head motion metric in this study. The scan was excluded if the head motion metric was  $>0.2$  mm. Here,  $n=8$ ,  $n=14$ , and  $n=48$  scans were further excluded, respectively, for the Calgary Preschool, HCP-D, and PNC datasets.
- (4) Functional connectome disconnection: To facilitate the S-T functional hierarchy analysis, we excluded the scans with disconnected functional connectivity (FC) matrix (refer to "Functional connectivity calculation"). Here,  $n=17$  and  $n=1$  scans were further excluded for the Calgary Preschool and PNC datasets, respectively.

Finally,  $n=141$ ,  $n=638$ , and  $n=795$  scans, respectively, for Calgary Preschool, HCP-D, and PNC datasets, were used for further analysis.

### FC calculation

After the preprocessing procedure, we calculated the FC matrix. Specifically, for the Calgary Preschool and PNC datasets, the preprocessed rs-fMRI time-series were resampled onto the conte69 surface space using workbench command (Marcus et al. 2013). We then averaged the time-series into 1,000-parcel cortical parcellation, as proposed by Schaefer et al. (2018). Notably, among the 1,000 parcels, two parcels were not available in the originally released label file. Then for each rs-fMRI scan, we calculated the FC matrix using Pearson's correlation, resulting in a  $998 \times 998$  FC matrix. For the HCP-D dataset, we first extracted cortical time-series from the preprocessed data. As the surface time-series were already in conte69 surface space, we applied the same cortical parcellation scheme (Schaefer et al. 2018) directly to it for each subject. After that, we calculated the FC matrix the same as above, and a  $998 \times 998$  FC matrix was obtained for each rs-fMRI scan.

### S-T functional hierarchy and its developmental pattern

For each FC matrix calculated above, an affinity matrix was further calculated using a cosine similarity kernel and then went through a row-wise 90% thresholding, followed by nonlinear dimensionality reduction implemented by diffusion map

embedding as in previous work (Margulies et al. 2016; Hong et al. 2019). Herein, we calculated the first 10 embeddings, resulting in a low-dimensional representation ( $998 \times 10$ ) for the original FC matrix ( $998 \times 998$ ) of each rs-fMRI scan. These embeddings were also known as functional hierarchies along different axes among which the S-T functional hierarchy of adults had been well characterized in a number of studies, including both healthy (Margulies et al. 2016) and psychiatric cohorts (Hong et al. 2019). The S-T functional hierarchy was anchored at one end by primary sensorimotor regions and default mode network (DMN) regions at the opposite end (Margulies et al. 2016). The above-mentioned procedure was conducted by the Brainspace toolbox (Vos de Wael et al. 2020).

We then aimed at investigating how the S-T functional hierarchy might develop with increasing age. Given that the adult cortical functional topography develops during the first 2 years of life (van den Heuvel et al. 2015), we aligned the low-dimensional representation of the functional connectome of the younger subjects to that of adults derived from an independent dataset (i.e. HCP 100 unrelated young adults (Hodge et al. 2016), age = 22–36 years, sex = 54F/46M) using the Procrustes alignment method (Langs et al. 2015). We focused on the first embedding (i.e. S-T functional hierarchy) after alignment. The GLM was then used to investigate age-related changes of the S-T functional hierarchy. For each of 998 parcels, we established a GLM with age as the independent variate, value of the S-T functional hierarchy as the dependent variate, and sex as a covariate. Notably, we observed that the head motion was negatively correlated with age, as was reported in Dong, Margulies, et al. (2021). Hence, the head motion was not included in the GLM in the main analysis. Besides, we evaluated the head motion effects by including head motion in the GLM as a covariate. The procedure provided us an age-related T statistical map for the following analysis.

### Functional annotation using the NeuroSynth database

Specific NeuroSynth terms were used to investigate the cognitive associates of the age-related T statistical map. NeuroSynth database (Yarkoni et al. 2011) contained 1,334 terms; however, the terms were restricted to those overlapped with the Cognitive Atlas (Poldrack et al. 2011) here, resulting in  $n=123$  terms for further analysis as in the previous studies (Shafiei et al. 2020; Hansen et al. 2021). See Supplementary File 1 for all the 123 terms used in this study. We used the "association test" volumetric maps, which were resampled to the conte69 surface space using workbench command (Marcus et al. 2013) and summarized across the 1,000-parcel cortical parcellation (Schaefer et al. 2018). This procedure yielded  $123$  (# of terms)  $\times$   $998$  (# of cortical parcels) maps. The age-related T statistical map was spatially correlated to the 123 NeuroSynth terms using Spearman's correlation, and the significance was determined by the permutation test (age permuted).

### Imaging transcriptomic analyses

Leveraging AHBA, we attempted to investigate microscale molecular mechanisms underlying the macroscale neuroimaging phenotype (i.e. developmental pattern of the S-T functional hierarchy). Since only the adult whole-brain transcriptome dataset is available, we evaluated the biological plausibility of spatial correlation between the adult gene expression map and the brain developmental pattern during childhood. Recently, Colantuoni et al. has reported that no dramatic changes of gene expression occur in the prefrontal cortex (PFC), after early childhood,



compared with that before birth and during infancy (Colantuoni et al. 2011). In this study, using the BrainSpan Atlas (refer to “Gene clustering based on developmental transcriptomic data from the BrainSpan Atlas” section), we further evaluated the gene expression temporal dynamics for other cortical areas (11 cortical regions, including PFC), and the results across multiple cortical areas were consistent with those of Colantuoni et al. (2011). See [Supplementary File 2](#) and [Supplementary Fig. 1](#) for further information.

### Transcriptomic data from the AHBA

AHBA is a high-resolution microarray transcriptomic dataset, including >20,000 gene expressions of 3,702 tissue samples obtained from 6 healthy adult donors (Hawrylycz et al. 2012). We downloaded the data from the AHBA website (<http://human.brain-map.org/>) and applied the abagen toolbox (Markello et al. 2021) to process and project the data into the 1,000-parcel cortical parcellation (Schaefer et al. 2018) using the default parameters. Briefly, microarray probe-to-gene mappings were reannotated with information from Amatkeviciute et al. (2019). The reannotated probes were then filtered by an intensity-based filtering method (i.e. only probes exceeding background noise in 50% of all tissue samples were retained). Then, among multiple probes corresponding to the same gene, the probe with the highest differential stability was selected. The above procedure yielded 15,631 genes. Following correction of the MNI coordinates (<https://github.com/chrisgorgo/alleninf>), the tissue samples were assigned to 998 parcels of the Schaefer’s parcellation scheme (Schaefer et al. 2018) by matching the nearest parcel (tolerance was 2 mm). The  $n=649$  parcels were assigned with at least 1 tissue sample. Tissue samples were then averaged separately for each donor and then averaged across the donors, resulting in a  $649$  (# of cortical parcels)  $\times$   $15,631$  (# of genes) gene expression matrix.

### Gene ranking

A total of 15,631 genes were ranked in descending order according to their expression correlations (Spearman’s correlation) with the S-T functional hierarchy developmental pattern (i.e. age-related T statistical map), resulting in the ranked gene list acting as the input for the subsequent enrichment analyses. See [Supplementary File 3](#) for the sorted gene list of Calgary Preschool, HCP-D, and PNC datasets.

### Definition of top-ranked genes

For the Calgary Preschool dataset, the top 5% of genes were selected as the top-ranked genes ( $n=782$ ). For the HCP-D and PNC datasets, we selected the overlapping genes of the 2 datasets’ top 10% genes as the top-ranked genes ( $n=452$ ) considering the age-range similarity and overall generalizability among these 2 datasets. Among the top-ranked genes from the Calgary Preschool dataset ( $n=782$ ),  $n=687$  genes were overlapped with the genes in the BrainSpan Atlas, while for the HCP-D and PNC datasets,  $n=406$  of the top-ranked genes (out of  $n=452$ ) were available in the BrainSpan Atlas. Notably, both the top 5% genes of Calgary Preschool dataset and the top 10% genes of HCP-D dataset survived FDR-BH procedure ( $P_{FDR} < 0.05$ ).

### Disease enrichment analysis

The Gene-Disease Associations (GDA), downloaded from the DisGeNET database (<https://www.disgenet.org/>; Piñero et al. 2020), were used to characterize the underlying disease enrichment profiles. We filtered GDAs based on the following 3 aspects:

- (1) Evidence index (EI): EI is an index that indicates the existence of contradictory results in the publications (e.g. EI = 1 indicates that all publications support the GDA). Herein, only the GDAs with EI = 1 were conserved.
- (2) Psychiatric disorders: If the disease of a GDA was marked as “Mental or Behavioral Dysfunction,” then this GDA was used for the disease enrichment analysis.
- (3) Availability in AHBA: If the gene of a GDA was not in the list of AHBA genes, then this GDA was removed.

After the procedure, 34,034 GDAs were retained, involving 747 psychiatric disorders. Finally, the disease enrichment analysis was conducted through fast preranked gene set enrichment analysis (FGSEA; Korotkevich et al. 2021) implemented by “clusterProfiler” R package (Wu et al. 2021), with the ranked gene list and 34,034 GDAs as the input.

### GO enrichment analysis

The top-ranked genes were submitted to ToppGene (<https://toppgene.cchmc.org/>) (Chen et al. 2009) to identify potentially relevant biological processes. The most significant twenty biological processes surviving the FDR-BH procedure ( $P_{FDR} < 0.05$ ) were displayed in our main results.

### Cell-type enrichment analysis

Two single-cell datasets were used in this study as follows:

- (1) Lake dataset: This single-nucleus droplet-based sequencing dataset (6 donors), reported by Lake et al. (2018), was derived from the postmortem adult human visual and frontal cortex samples. Notably, lateral cerebellar samples of the dataset were not considered in our analyses, as this study focused on the cerebral cortex.
- (2) Allen Brain Institute (ABA) dataset: This single-nucleus ribonucleic acid (RNA) sequencing dataset (8 donors) was developed by the ABA (Hodge et al. 2019) from intact nuclei derived from frozen brain specimens of adult human middle temporal gyrus.

Using the Seurat R package (Stuart et al. 2019), we applied the same preprocessing steps as previously published by Anderson et al. (2020) to the above-mentioned datasets. Specifically, genes expressed in <3 cells and cells with expressed genes of <200 were removed. Then, the expression values were log-normalized, followed by covariates (i.e. sequencing platform and processing batch) regression and data scaling. Predefined 8 cell types of the Lake dataset (excitatory neurons [Exc], inhibitory neurons [Inh], astrocyte [Ast], oligodendrocyte [Oli], pericyte [Per], endothelial [End], microglia [Mic], and oligodendrocyte precursor cell [OPC]) and 7 cell types of ABA dataset (Exc, Inh, Ast, Oli, End, Mic, and OPC) were used for the following cell enrichment analysis separately. Gene markers for each cell type were determined via the Wilcoxon Rank-Sum test (Bonferroni correction,  $P_{Bonf} < 0.05$ ).

A hypergeometric test was used to further investigate the cell-type enrichment profiles of the top-ranked genes. See [Supplementary File 2](#) for further information.

### Gene clustering based on developmental transcriptomic data from the BrainSpan Atlas

After exploring the GO, disease, and cell-type enrichment profiles of the top-ranked genes, we were interested in examining whether these genes, based on their temporal expression trajectories, could be classified into specific clusters, where each cluster was attached with specific GO terms, disease, and cell-type. To do so, we used the cortical RNA-sequencing (RNA-seq) data from

the BrainSpan Atlas (<http://www.brainspan.org>) to characterize the developmental trajectories of the top-ranked genes. The BrainSpan Atlas dataset is an RNA-seq gene expression dataset with high temporal resolution (31 ages, ranging from 8 post-conception weeks to 40 years;  $n=11$  cortical regions). The gene expression was averaged across the 11 cortical regions, followed by log2 transformation and scaling. This provided us with a 31 (# of ages)  $\times$  52,376 (# of genes) gene expression matrix. Based on this developmental gene expression matrix, the top-ranked genes were clustered using mixed-effects models with nonparametric smoothing spline fitting implemented in the TMixClust R package (Golumbeanu 2021). Silhouette width (Rousseeuw 1987) was utilized to determine the optimal number of clusters (from  $K=2$  to  $K=6$ ). The optimal clustering solution was then determined by 20 iterations, and agreements between the iterations were evaluated by the rand index (Hubert and Arabie 1985). See [Supplementary File 2](#) for details of definition/denotation of the resulting gene clusters. Following that, for each cluster of the top-ranked genes, we conducted the identical enrichment analyses as described above (i.e. “Disease enrichment analysis”, “GO enrichment analysis”, and “Cell-type enrichment analysis”). Notably, as the genes of interest were a subset of the ranked gene list, the disease enrichment analysis was conducted using a hypergeometric test as described in the “Cell-type enrichment analysis” section and [Supplementary File 2](#).

## Statistical analyses

Age-related T map was generated by the GLM implemented in the python package statsmodels (Seabold and Perktold 2010). Specifically, the T value for each parcel was calculated as the slope (i.e.  $\beta_{\text{age}}$ ) divided by its standard error. The significance for the associations between the S-T functional hierarchy developmental pattern and the NeuroSynth term maps were evaluated by randomly permutating the ages 1,000 times ( $P_{\text{perm}} < 0.05$ ), which reflected the age-related effects on our findings as well. The significance of disease and GO enrichment was evaluated by applying the FDR-BH multiple correction procedure ( $P_{\text{FDR}} < 0.05$ ). Gene markers for each cell type were determined via the Wilcoxon Rank-Sum test (Bonferroni correction,  $P_{\text{Bonf}} < 0.05$ ), and a hypergeometric test was utilized to test the significance of the overlap between the gene sets in the cell-type enrichment analysis ( $P_{\text{hyper}} < 0.05$ ).

## Results

### Developmental pattern of the S-T functional hierarchy in preschool children

We first examined the developmental pattern of S-T functional hierarchy in 141 passive viewing fMRI scans (age = 2.41–6.90 years) from the Calgary Preschool dataset by using the GLM model with value of S-T functional hierarchy as the dependent variate, age as the independent variate, and sex as a covariate. The age-related T statistical map from the GLM model ([Fig. 1A](#)) showed that the S-T functional hierarchy values corresponding to the transmodal regions increased and that those of the sensorimotor regions decreased with increasing age in preschool children. These results were consistent when head motion was included as a covariate in GLM (Spearman’s  $r=0.97$ ,  $P_{\text{perm}} < 0.001$ , age permuted 1,000 times, [Supplementary Fig. 2](#)). Then, we investigated the age-related changes in the functional brain networks by collapsing the age-related T statistical map into Yeo-7 networks, which showed that changes in the higher-order transmodal networks (e.g. DMN) hierarchy were positive and those in the primary sensorimotor networks (e.g. somatosensory network) were negative during

early development ([Fig. 1C](#)), further supporting the fact that the functional segregation of brain networks occurred during this developmental period. Median values of S-T functional hierarchy between the older and the younger groups across the Yeo-7 networks showed that the “preschool older group” occupied more wide-spread values at the terminals (i.e. higher values in the transmodal networks and lower values in the somatosensory networks) compared with the “preschool younger group” ([Fig. 1D](#)). Moreover, we investigated the relevant cognitive profiles of the S-T functional hierarchy developmental pattern by analyzing the associations between the age-related T map and NeuroSynth term maps, which revealed that the development of the S-T functional hierarchy was positively associated with higher-order cognitive functions, such as memory retrieval, decision making, and inference, while being negatively associated with motion and sensation in particular (all terms survived permutation test  $P_{\text{perm}} < 0.05$  are shown in [Fig. 1B](#), age permuted 1,000 times). Together, these results supported our hypothesis that the S-T functional hierarchy in preschool children could gradually develop into a more distinct and complex hierarchy, with the higher-order transmodal regions further segregated from the primary sensorimotor regions under healthy conditions.

### Transcriptomic characteristics of the S-T functional hierarchy developmental pattern

To understand the underlying mechanisms driving the developmental pattern of S-T functional hierarchy, we ranked the genes in descending order by Spearman’s correlation coefficient values between the age-related T map and their expression maps from the AHBA dataset ([Fig. 2A](#)) and subsequently performed disease, GO, and cell-type enrichment analyses on the ranked gene list (15,631 genes). GSEA for psychiatric disorders resulted in 16 significantly enriched disorders ([Fig. 2B](#)), consisting of ASD, cocaine-related disorders, etc. We found that the normalized enrichment scores (NESs) of these 16 disorders were all positive, suggesting that top-ranked genes might play more critical roles in neurodevelopmental disorders compared with the bottom-ranked genes. We then selected the top 5% genes ( $n=782$ ) to conduct overrepresentation analysis (ORA) for GO terms using Toppgene ([Chen et al. 2009](#)). Our results showed that cellular process-related terms (e.g. synaptic signaling and signal release) and developmental process-related terms, like neuron differentiation, were significantly enriched for these genes (all FDR-BH-corrected  $P_{\text{FDR}} < 0.05$ ; the top twenty enriched items are shown in [Fig. 2C](#) and all significantly enriched GO items are listed in [Supplementary File 4](#)). By contrast, the bottom 5% genes were not significantly enriched in any GO terms. We then conducted ORA for 8 cell types, defined by [Lake et al. \(2018\)](#), and found that the top 5% genes were enriched in the Exc and Inh (Exc: hypergeometric test  $P_{\text{hyper}} = 3.77 \times 10^{-5}$ ; Inh: hypergeometric test  $P_{\text{hyper}} = 0.02$ ). These findings were recapitulated in the case of 7 cell types predefined in the ABA dataset (see [Supplementary Fig. 3](#) for the Lake dataset and [Supplementary Fig. 4](#) for the ABA dataset).

### Clustering of the S-T functional hierarchy development-related genes

It has been well established that the gene expression patterns are prone to dynamic changes over time, especially at different developmental stages ([Colantuoni et al. 2011](#); [Kang et al. 2011](#)). To characterize the gene expression dynamics, we clustered the top 5% genes according to their temporal expression trajectories into two groups ([Fig. 3A](#)). See [Supplementary File 2](#) and [Supplementary Figs. 6–9](#) for the definition procedure of the two gene clusters.

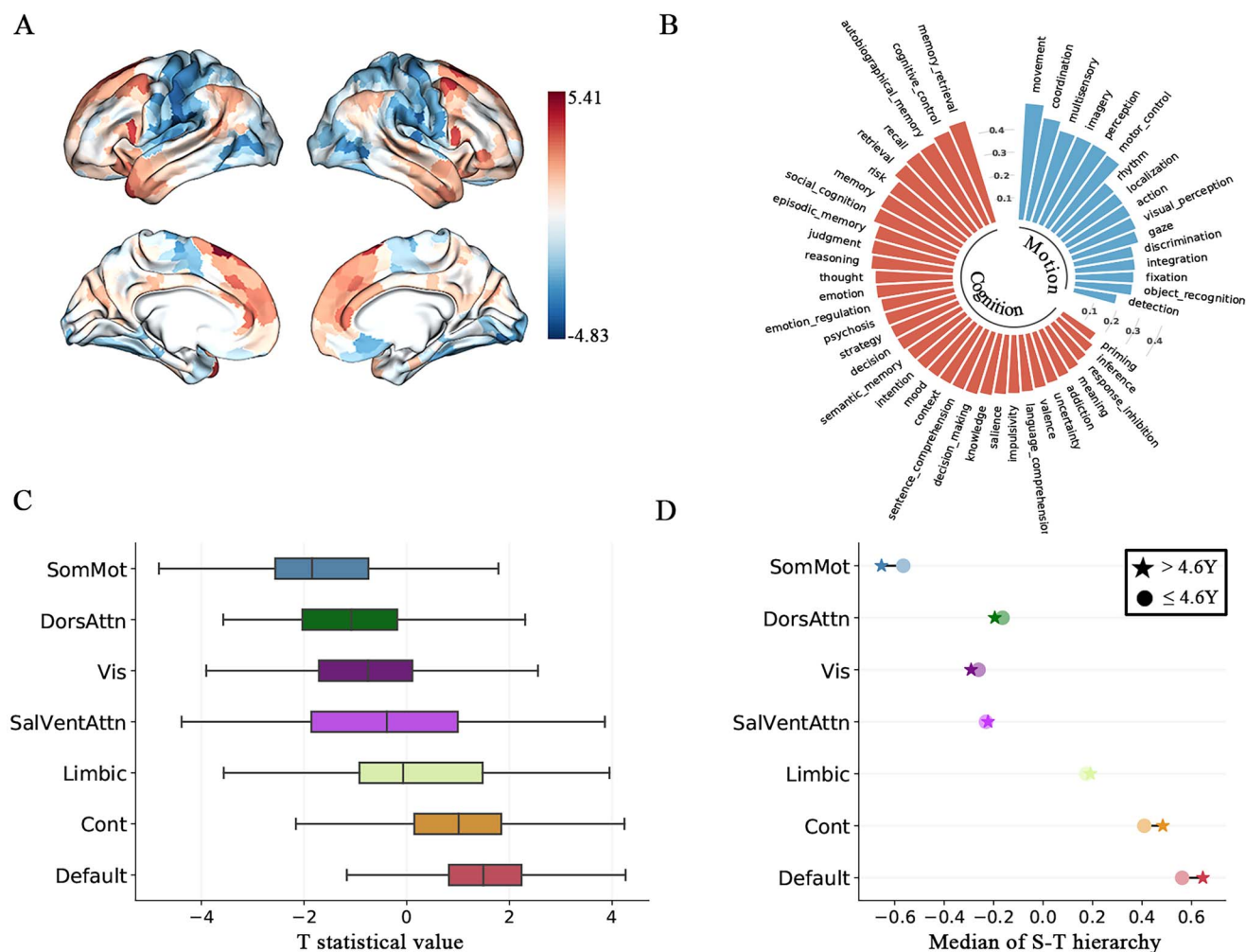


**Fig. 1. Developmental pattern of the S-T functional hierarchy in preschool children.** **A)** Age-related T statistical map derived from the GLM. Age-related increases were primarily clustered in the transmodal regions, while the decreases were in the sensorimotor regions. Here, the head motion was not included in the GLM. See [Supplementary Fig. 2](#) for the results when including the head motion in the GLM. **B)** Functional annotation of the age-related statistical T map (A) using the NeuroSynth database. The length of the bars indicated the absolute correlation values (Spearman's) between the age-related statistical T map and the NeuroSynth terms. Red: positive correlation, blue: negative correlation. Positive correlations occurred mainly in the cognition/mood-related terms; negative correlations were held primarily in the motion-/sensation-related terms. All terms that survived the age permutation test ( $P_{\text{perm}} < 0.05$ ) are shown. See [Supplementary File 1](#) for all NeuroSynth terms used in this study ( $n = 123$ ). **C)** Age-related T statistical map (A) collapsed into Yeo-7 functional networks. The box plot was ordered by median values. **D)** The lollipop plot displayed the median of S-T functional hierarchy values across Yeo-7 functional networks for the “> 4.6Y” group (“preschool older group,” indicated by a pentagram) and “≤ 4.6Y” group (“preschool younger group,” indicated by a circle). Note: 4.6Y was the median age of the Calgary Preschool dataset. The “SomMot” and “Default” networks showed an extending trend during development. SomMot: somatomotor network, DorsAttn: dorsal attention network, Vis: visual network, SalVentAttn: salience ventral attention network, Limbic: limbic network, Cont: frontoparietal control network, Default: default network.

Intriguingly, we noticed that genes of one cluster (denoted as “prenatal”, the blue line in [Fig. 3A](#)) were preferentially expressed during the prenatal periods, while genes of another cluster (denoted as “postnatal”, the red line in [Fig. 3A](#)) were expressed at the highest level during the postnatal periods. We then performed the identical enrichment analyses for the two clusters separately. Disease enrichment analysis showed that the prenatal cluster ([Fig. 3B](#), blue line) was enriched in ASD, while the postnatal cluster ([Fig. 3B](#), red line) was enriched in various addiction disorders, such as cocaine dependence. Furthermore, GO enrichment analysis revealed that the prenatal cluster was mostly associated with the developmental process-related terms (e.g. neuron differentiation and neurogenesis), while the postnatal cluster was mostly enriched in cellular process-related terms (e.g. synaptic signaling and chemical synaptic transmission; in [Fig. 3C](#), and the

20 terms shown are the same as those of [Fig. 2C](#). See [Supplementary File 5](#) for all significantly enriched GO terms of the prenatal cluster and [Supplementary File 6](#) for the postnatal cluster). Cell-type enrichment analysis ([Fig. 3D](#)) indicated that the prenatal cluster was enriched in Inh (hypergeometric test,  $P_{\text{hyper}} = 0.02$ ), while the postnatal cluster was enriched in Exc (hypergeometric test,  $P_{\text{hyper}} = 7.22 \times 10^{-6}$ ).

In addition, these findings were independently replicated in the ABA dataset (see [Supplementary Fig. 5](#)). Collectively, our results suggested that the two clusters of genes with distinct developmental expression trajectories were involved in different diseases, GO terms, and cell types. Thus, the consideration of temporal gene expression trajectories could be critical for identifying the potential genetic factors in neurodevelopmental diseases apart from spatial gene expression profiles.



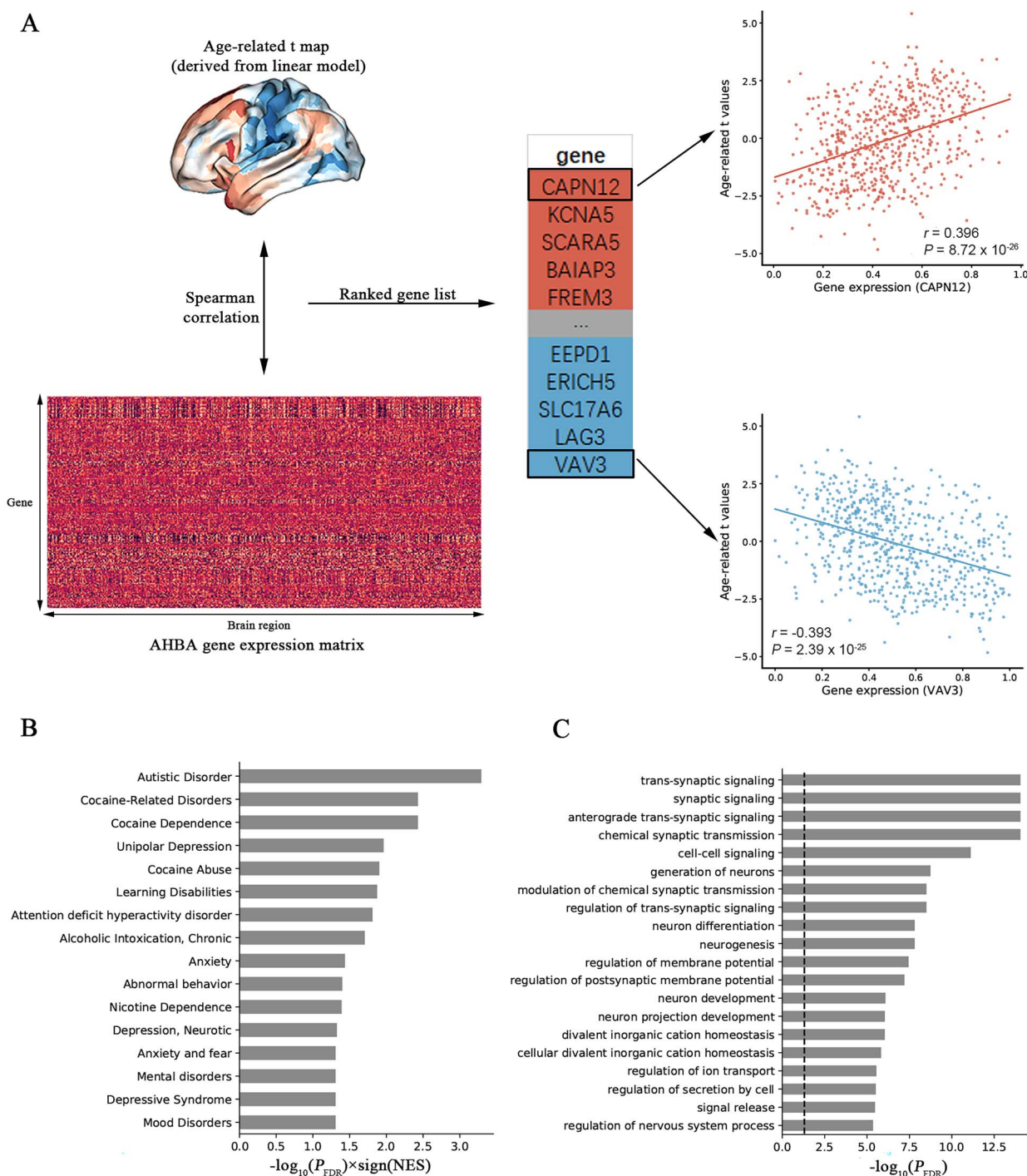


**Fig. 2. Transcriptomic characteristics of the S-T functional hierarchy developmental pattern.** **A)** Schematic workflow combining the neuroimaging developmental pattern with the AHBA dataset. A total of 15,631 genes were sorted by correlation (Spearman's) between their respective gene expression patterns from AHBA and the age-related T statistical map in descending order. Genes with the more positive correlation ranked top. See [Supplementary File 3](#) for the sorted gene list of Calgary Preschool, HCP-D, and PNC datasets. **B)** Disease enrichment profiles of the ranked gene list. All significantly enriched diseases were shown. All the diseases were positively enriched, suggesting the importance of the top-ranked genes. **C)** GO enrichment profiles of the top 5% genes from the ranked gene list. The most significant twenty GO terms were displayed. See [Supplementary File 4](#) for all significantly enriched GO terms.

## Extrapolation to consecutive developmental stages

We then attempted to examine whether the observed patterns and relevant molecular profiles of the S-T functional hierarchy development in preschool children were developmental

stage-dependent by conducting the identical analyses in two independent developmental datasets, including the HCP-D ( $n = 638$  scans, age = 5.58–21.92 years, sex = 346F/292M) and PNC datasets ( $n = 795$  scans, age = 8–21 years, sex = 429F/209M). As expected, we found that the age-related T statistical map

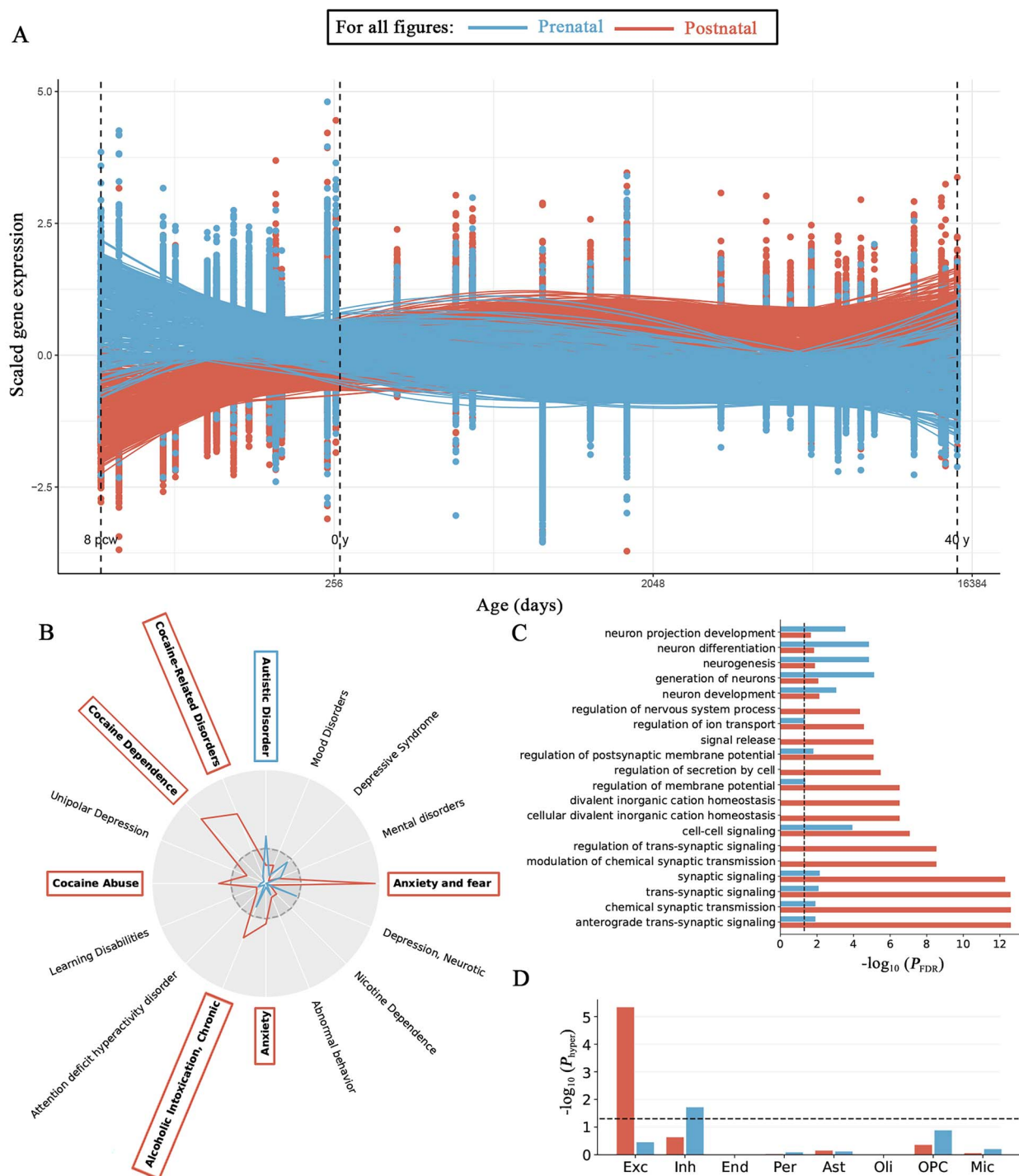


**Fig. 3. Clustering of the S-T functional hierarchy development-related genes.** Note: for all subfigures of this figure, blue represents the prenatal cluster, while red indicates the postnatal cluster. **A)** Gene expression trajectories for the top 5% genes ( $n=687$ ) from the ranked gene list. The LOESS fitted lines were shown, and the color represented cluster assignment. **B)** Radar plot showed the disease enrichment profiles for the prenatal cluster (blue) and the postnatal cluster (red), with the dashed circle indicating that the hypergeometric  $-\log_{10}(P_{\text{hyper}}) = 1.30$  (i.e.  $P_{\text{hyper}} = 0.05$ ). Diseases surviving the hypergeometric test ( $P_{\text{hyper}} < 0.05$ ) were those exceeding the dashed circle. **C)** GO enrichment profiles for the prenatal cluster and the postnatal cluster. The displayed twenty terms were the same as those in Fig. 2C. Dashed line represents that  $-\log_{10}(P_{\text{FDR}}) = 1.30$  (i.e.  $P_{\text{FDR}} = 0.05$ ). See Supplementary File 5 for all significantly enriched GO terms for the prenatal cluster and Supplementary File 6 for the postnatal cluster. **D)** Cell-type enrichment profiles for the prenatal cluster and the postnatal cluster using the Lake dataset. Dashed line represented that  $-\log_{10}(P_{\text{hyper}}) = 1.30$  (i.e.  $P_{\text{hyper}} = 0.05$ ). See Supplementary Fig. 5 for results from the ABA dataset.

for the S-T functional hierarchy of the two datasets were significantly correlated with that of the Calgary Preschool dataset (HCP-D:  $r=0.39$ ,  $P_{\text{perm}}=0.002$ , age permuted 1,000 times, Fig. 4A; PNC:  $r=0.35$ ,  $P_{\text{perm}}=0.003$ , age permuted 1,000

times, Fig. 4B), suggesting that the S-T functional hierarchy may gradually develop at a similar pace in children and adolescents compared with preschool children. (Notably, the spatial association between the developmental patterns derived



from HCP-D and PNC datasets was more prominent [ $r=0.47$ ,  $P_{\text{perm}} < 0.001$ , [Supplementary Fig. 10](#)], suggesting the existence of some early childhood-specific changes. See [Supplementary File 2](#), [Supplementary Fig. 11](#) for further information.) The ranked gene lists for these 2 datasets were first obtained by independently performing imaging transcriptomic analyses, which was followed by the disease enrichment analysis revealing that the NESs of enriched diseases for both the HCP-D and PNC datasets were positive (see [Supplementary File 7](#) for the HCP-D dataset and [Supplementary File 8](#) for the PNC dataset), suggesting that the top-ranked genes should be selected for further analysis. Using the temporal expression profiles extracted from the BrainSpan Atlas, we then clustered the new top-ranked genes into two groups ([Fig. 4C](#)) and characterized them as prenatal genes' and postnatal genes' groups as found in the Calgary Preschool dataset. Notably, the functional annotations of the 2 clusters were also highly concordant with those of the Calgary Preschool dataset ([Fig. 4D and E](#)). Specifically, the prenatal cluster was enriched in the developmental process-related GO terms, such as "neuron differentiation," while the postnatal cluster was enriched in the cellular process-related GO terms, such as "response to toxic substance" and "signal release."

## Discussion

Our findings showed that the hierarchical organization of the functional connectome could be a highly dynamic and complex system, which exhibited a broad range of maturation and differentiation processes in both unimodal and transmodal cortical regions, as established in terms of the S-T functional hierarchy segregation along the various neurodevelopmental stages. Leveraging the imaging transcriptomic analyses of spatio-temporal expression patterns of the neurodevelopment-related genes, we intriguingly found two independent gene clusters with high prenatal or postnatal expression profiles, which might drive the long-term development of the S-T functional hierarchy as compared among three independent datasets. These findings provided a comprehensive developmental principle of cortical S-T functional hierarchy and helped us understand the underlying molecular mechanisms that might play pivotal roles in the complex functional segregation processes of the hierarchical cortical networks.

One of the major findings of the present study was the gradual development of cortical S-T functional hierarchy from the age of 2 years to early adulthood by embedding the functional brain network analysis across three independent datasets. Previous anatomical and functional evidence has supported the fact that cortical topography found in adults is (partly) present in the very early developmental stage, as the initiation point to develop the brain circuit into a more "adult-like" state during the subsequent developmental processes ([Hagmann et al. 2010](#); [Li et al. 2015](#); [van den Heuvel et al. 2015](#)). Specifically, sensorimotor networks are largely established even before birth and undergo subtle changes later, while the transmodal networks, present at birth in an immature form, are similar to those of adulthood in a 2-year-old as well ([Gao et al. 2009](#); [Gao, Alcauter, Elton, et al. 2015](#)). Therefore, these findings suggest the existence of the fundamental organization of functional brain networks by the age of 2 years. Interestingly, we found the most significant changes in age-related S-T functional hierarchy at the two extreme ends, namely, sensorimotor regions and transmodal regions, indicating that transmodal regions were further segregated from sensorimotor regions during the development. Studies have highlighted the segregation of the cortical functional networks as an important

process for complex cognitive functions ([Dosenbach et al. 2010](#); [Gu et al. 2015](#)). In our study, a similar developmental pattern of the S-T functional hierarchy was observed in the subsequent development periods (i.e. late-childhood and early adulthood) in both HCP-D and PNC datasets, which was in agreement with previous findings ([Nenning et al. 2020](#); [Xia et al. 2022](#)). Besides, [Dong, Margulies, et al. \(2021\)](#) have reported that the S-T functional hierarchy gradually shifts to be the principal hierarchy, suggesting that this specific functional hierarchy explained much more variance of the functional connectome during the developmental reorganization of the functional networks in the brain, further supporting our results. Furthermore, the functional annotations using the NeuroSynth database ([Yarkoni et al. 2011](#)) were consistent with the roles of functional networks, like positive associations (dominant in the transmodal regions) with cognition-/mood-related terms and negative associations (dominant in the sensorimotor regions) primarily with sensation-/motion-related terms, thus emphasizing the segregation of brain networks.

Our findings based on imaging transcriptomic analyses revealed the critical molecular mechanisms underlying the cortical S-T functional hierarchy development. Specifically, disease enrichment analysis suggested that the top-ranked genes associated with the S-T functional hierarchy development were enriched primarily in the ASD, cocaine-related disorders, etc. Intriguingly, [Hong et al.](#) have found that the S-T functional hierarchy in the ASD cohorts, although manifested similar bimodal distribution, was globally contracted compared with the healthy controls ([Hong et al. 2019](#)), further supporting the importance of segregation between sensorimotor and transmodal regions during typical brain development. Additionally, at the cellular level, our cell-type specific enrichment analyses revealed that these S-T functional hierarchy development-related genes were significantly enriched in Exc and Inh, the interaction of which is crucial for typical cortical development, potentially pointing to the excitation:inhibition (E:I) ratio imbalance in neurodevelopmental disorders ([Rubenstein and Merzenich 2003](#)). For example, a recent study has verified typical reductions of the E:I ratio during typical cortical development, which are associated with individual differences in mood disorder symptomatology as well ([Larsen et al. 2022](#)). The developmental reductions in E:I ratio result in an increase in the signal-to-noise ratio of neural circuits, facilitating more efficient information processing. The abnormal increase of E:I ratio, in contrast, leading to the reduction of signal-to-noise ratio, has been linked to neurodevelopmental disorders such as ASD and schizophrenia ([Canitano and Pallagrosi 2017](#); [Sohal and Rubenstein 2019](#); [Markicevic et al. 2020](#)). At the molecular level, the GO enrichment analyses suggested that the S-T functional hierarchy development-related genes were enriched in developmental process-related and cellular process-related GO terms, such as "neuron differentiation" and "synaptic signaling," consistent with the evidence that the orchestration activity of genes related to such biological processes is crucial for typical cortical development ([Richiardi et al. 2015](#); [Subramanian et al. 2020](#)), and any disruptions may lead to neurodevelopmental disorders such as ASD ([Zoghbi and Bear 2012](#); [Parenti et al. 2020](#)). Moreover, recent studies on cortical thickness developmental patterns combined with the gene enrichment analysis have also reported the involvement of similar GO terms and specific neurons ([Ball et al. 2020](#); [Patel et al. 2021](#)), suggesting the possible overlapping molecular mechanisms underlying cortical structural and functional development.

Another intriguing finding in the present study was that the cortical S-T functional hierarchy development-related genes

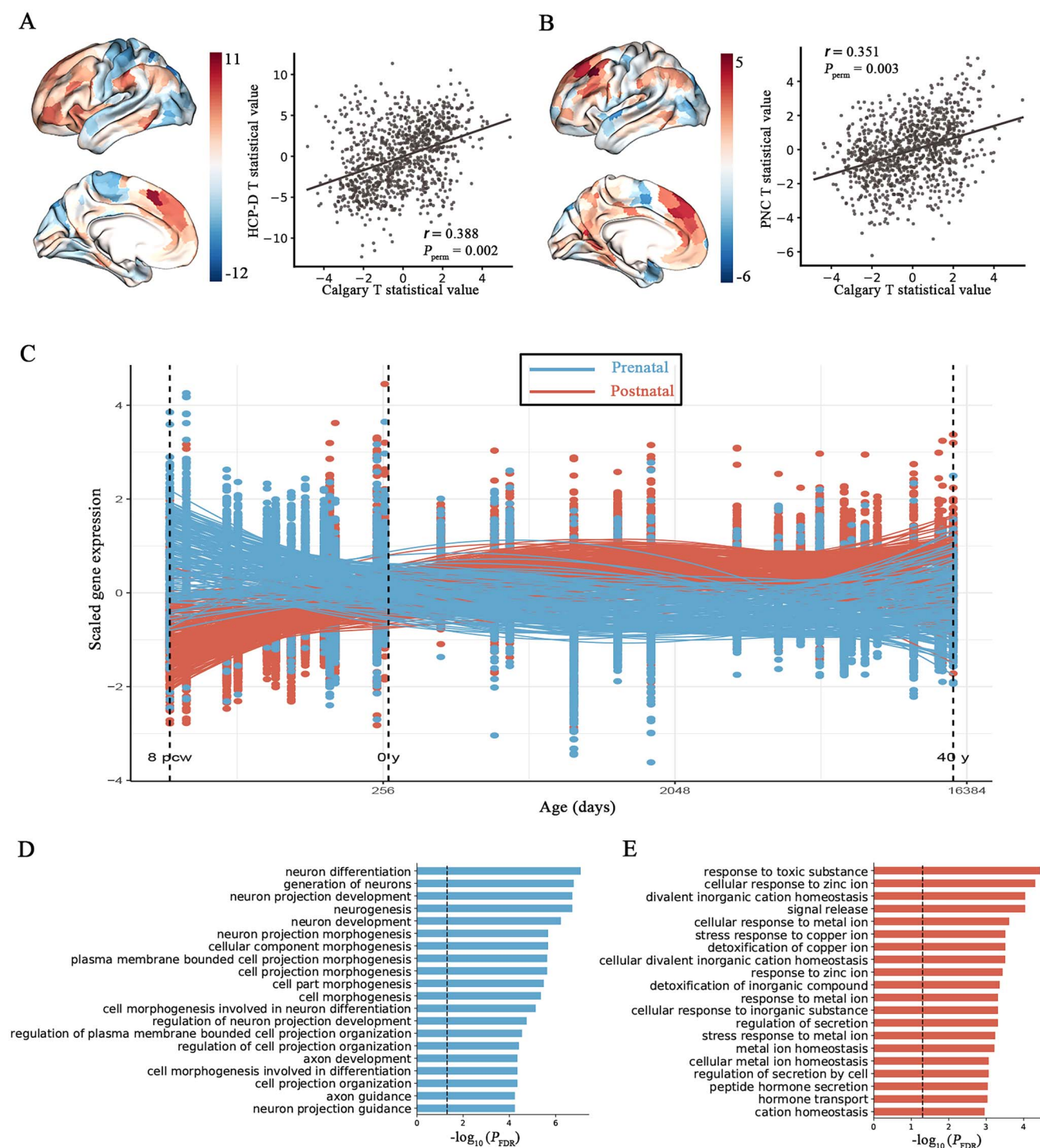


**Fig. 4. Extrapolation to consecutive developmental periods.** **A)** Age-related T statistical map for HCP-D dataset (left) and the scatter plot showed its correlation (Spearman's) with that of the Calgary Preschool dataset (right). **B)** Age-related T statistical map for PNC dataset (left) and the scatter plot showed its correlation (Spearman's) with that of the Calgary Preschool dataset (right). **C)** Gene expression trajectories for the overlapped genes between the top 10% genes from HCP-D and PNC datasets. The LOESS fitted lines were shown and the color represented cluster assignment. Blue represents the prenatal cluster, while red represents the postnatal cluster. **D)** GO enrichment profiles for the prenatal cluster. See [Supplementary File 9](#) for all significantly enriched GO terms. **E)** GO enrichment profiles for the postnatal cluster. See [Supplementary File 10](#) for all significantly enriched GO terms.

perfectly fell into two categories (preferentially prenatal or postnatal expressed gene clusters) according to their developmental expression profiles. Previous studies have indicated that the gene expression discrepancies between the prenatal and postnatal periods explain as much as 2/3 of the global expression variance (Silbereis et al. 2016), suggesting that the prenatal and postnatal

genes might express differentially, making mutually exclusive and critical contributions to the functional segregation during the cortical development. Specifically, the prenatal gene cluster was found to be enriched in the developmental process-related GO terms, such as “neurogenesis” and “neuron differentiation,” consistent with the biological characteristics of the prenatal period

(i.e. more intrinsically regulated). Such biological processes were important for cortical wiring early in life (Metcalfe et al. 1990), subtle perturbations of which may cascade onto the long-term impact on function of the brain and further result in an increased susceptibility to many neurodevelopmental disorders in later life (O'Donnell and Meaney 2017). Notably, prenatal disruptions of cortical circuits have already been verified, in previous animal studies, to be associated with neurodevelopmental disorders such as ASD, schizophrenia, and intellectual disability (Lavin et al. 2005; Lodge and Grace 2009; Kozol 2018). Interestingly, our disease enrichment analyses also indicated that the prenatal gene cluster was enriched in ASD, verifying the previous postmortem findings that risk genes of neurodevelopment disorders such as ASD are relatively upregulated in prenatal periods as well (Birnbau et al. 2014). Moreover, we also found that the prenatal genes were enriched in Inh, conforming to the increasingly supported hypothesis that disruptions of inhibitory interneurons underlie neurodevelopmental disorders (Chen et al. 2020) as the E:I ratio balance is critical for the cortical circuits' maintenance (Sohal and Rubenstein 2019). Given that atypical S-T functional hierarchy has been reported in ASD (Hong et al. 2019), our findings may shed light on the potential underlying molecular mechanisms. Taken together, we hypothesize that the prenatal genes may mainly regulate cortical patterning at the very beginning, establishing the backbone for subsequent typical cortical development.

By contrast, the postnatal genes were enriched in cellular process-related GO terms, such as "synaptic signaling" and "chemical synaptic transmission." Such biological processes, reflecting processes important in the postnatal cortical development, have been associated with the functional connectome in the human brain (Richiardi et al. 2015). Moreover, analogous biological processes serve as the basis for synapse pruning (Sakai 2020; Faust et al. 2021). The synapse pruning, largely facilitating the remodeling of cortical circuits, is a highly experience-driven process (Tierney and Nelson 2009). Interestingly, our disease enrichment analyses revealed that the postnatal genes were enriched in various addiction disorders, such as cocaine abuse, which was more specific to and can be eliminated by daily experiences and environmental factors (Solinas et al. 2008), possibly reflecting the plasticity of cortical circuits in postnatal periods. Moreover, we found that the postnatal cluster was enriched in Exc, which is consistent with the view that excitatory synapses were important for environmental response-related activities such as learning and memory (Froemke 2015). Furthermore, previous studies have also demonstrated that the uncontrollable desire for drugs in addiction arises from pathological manifestations of neuroplasticity in excitatory transmission (Thomas et al. 2001; Winder et al. 2002). In summary, we speculate that the postnatal genes, involved in plasticity-related processes, may be crucial in cortical remodeling in postnatal periods.

Although our findings are likely to provide potential clues about the complex processes of cortical development and the underlying molecular mechanisms, the involvement of certain limitations should be carefully considered. First, using the microarray gene expression data (i.e. AHBA) from six adult postmortem brains to infer associations with neuroimaging developmental phenotypes in early childhood harbored some scientific uncertainty and could be confounded by age-related changes in gene expressions. Our current findings are under the hypothesis that the gene expression profiles in early childhood may be analogous to that in adulthood, as in previous studies

(Ortiz-Terán et al. 2017). Future studies using age-matched gene expression data, if available, should seek to replicate our findings. Second, cortical functional development is a complex process, which may not necessarily be fully captured by a linear model. Here, we selected the linear model, considering statistical power following previous studies (Gao, Alcauter, Smith, et al. 2015; Nenning et al. 2020). Other nonlinear models may be applied in future studies to further validate these results. Moreover, the S-T functional hierarchy is one simplified representation, among many others, of the cortical functional connectome. For example, another hierarchy, where cortical features are differentiated between the sensorimotor modalities (e.g. visual regions vs. motor regions), has also been described in previous studies (Margulies et al. 2016; Huntenburg et al. 2018). Further investigations of other cortical features over time are warranted to advance our understanding of cortical development. Third, our findings were derived from three independent cross-sectional datasets. The cross-sectional datasets, however, are limited in the ability to examine within-individual variabilities (King et al. 2018). Thus, further validation in the longitudinal developmental cohorts is warranted. Fourth, for the pediatric cohorts, the head motion was a critical concern. During the evaluation of the impact of brain development stages on neuroimaging phenotypes, head motion was significantly correlated with increasing age in general. Therefore, untangling the motion effects was difficult. Moreover, Zeng et al. have found that motion-related differences reflect a neurobiological trait instead of pure motion artifacts and that the trait remains stable across time (Zeng et al. 2014). Therefore, we explored the developmental pattern with and without the inclusion of head motion in the model separately and found that the patterns were correlated significantly with each other. However, how to reasonably deal with the head motion remains elusive. Besides, the brain template for preprocessing pipeline for very young subjects needs more focus. Use of the MN152 template, usually utilized for adults, could induce technical biases. Therefore, a pediatric template derived from  $n=324$  subjects of 4.5–18.5 years (Fonov et al. 2011) of age range was used in our study. In the future, leveraging finer templates may be helpful in capturing the age-related changes while reserving the age-specific features. Fifth, as is common with previous imaging transcriptomic studies (Whitaker et al. 2016; Ortiz-Terán et al. 2017; Morgan et al. 2019), our cross-scale findings are correlational in nature. Although imaging transcriptomic analyses have been verified, to some extent, in terms of its validity (Martins et al. 2021), our associative conclusions should be cautiously interpreted and biologically validated in the future. Moreover, the clinical relevance of the prenatal/postnatal gene clusters may be further explored in future studies, aiding in early screening and intervention for neurodevelopment disorders.

## Conclusion

In summary, the main findings of our work were twofold. First, from the macroscale neuroimaging perspective, we found consistent functional segregated characteristics of the S-T functional hierarchy during development, using three developmental datasets across a large age interval. Second, from the cross-scale perspective (i.e., by integrating macroscale neuroimaging pattern and microscale molecular information), leveraging spatiotemporal transcriptomic datasets, we found the above-mentioned macroscale pattern may be potentially driven by two distinct molecular profiles manifested in prenatal/postnatal



periods (trait-like versus activity-dependent). Such findings may reveal intrinsic cortical developmental principles and provide critical insights into the etiology of neuropsychiatric and neurodevelopmental disorders such as ASD.

## Supplementary material

Supplementary material is available at *Cerebral Cortex* online.

## Funding

This work was supported by the National Natural Science Foundation of China (Grant number 81771451) and the Startup Funds of Beijing Normal University.

Conflict of interest statement: None declared.

## References

- Anderson KM, Collins MA, Kong R, Fang K, Li J, He T, Chekroud AM, Yeo BTT, Holmes AJ. Convergent molecular, cellular, and cortical neuroimaging signatures of major depressive disorder. *Proc Natl Acad Sci U S A*. 2020;117(40):25138–25149.
- Arnatkeviciute A, Fulcher BD, Fornito A. A practical guide to linking brain-wide gene expression and neuroimaging data. *NeuroImage*. 2019;189:353–367.
- Ball G, Seidlitz J, Beare R, Seal ML. Cortical remodelling in childhood is associated with genes enriched for neurodevelopmental disorders. *NeuroImage*. 2020;215:116803–116816.
- Bertolero MA, Blevins AS, Baum GL, Gur RC, Gur RE, Roalf DR, Satterthwaite TD, Bassett DS. The human brain's network architecture is genetically encoded by modular pleiotropy. 2019: arXiv:190507606 [q-bio].
- Birnbaum R, Jaffe AE, Hyde TM, Kleinman JE, Weinberger DR. Prenatal expression patterns of genes associated with neuropsychiatric disorders. *AJP*. 2014;171(7):758–767.
- Buckner RL, Krienen FM. The evolution of distributed association networks in the human brain. *Trends Cogn Sci*. Special Issue: The Connectome. 2013;17(12):648–665.
- Burt JB, Demirtaş M, Eckner WJ, Navejar NM, Ji JL, Martin WJ, Bernacchia A, Anticevic A, Murray JD. Hierarchy of transcriptomic specialization across human cortex captured by structural neuroimaging topography. *Nat Neurosci*. 2018;21(9):1251–1259.
- Canitano R, Pallagrosi M. Autism spectrum disorders and schizophrenia spectrum disorders: excitation/inhibition imbalance and developmental trajectories. *Front Psych*. 2017;8:69.
- Chen J, Bardes EE, Aronow BJ, Jegga AG. ToppGene suite for gene list enrichment analysis and candidate gene prioritization. *Nucleic Acids Res*. 2009;37(Web Server):W305–W311.
- Chen C-H, Gutierrez ED, Thompson W, Panizzon MS, Jernigan TL, Eyler LT, Fennema-Notestine C, Jak AJ, Neale MC, Franz CE, et al. Hierarchical genetic organization of human cortical surface area. *Science*. 2012;335(6076):1634–1636.
- Chen C-H, Fiecas M, Gutierrez ED, Panizzon MS, Eyler LT, Vuoksima E, Thompson WK, Fennema-Notestine C, Hagler DJ, Jernigan TL, et al. Genetic topography of brain morphology. *Proc Natl Acad Sci U S A*. 2013;110(42):17089–17094.
- Chen Q, Deister CA, Gao X, Guo B, Lynn-Jones T, Chen N, Wells MF, Liu R, Goard MJ, Dimidschstein J, et al. Dysfunction of cortical GABAergic neurons leads to sensory hyper-reactivity in a Shank3 mouse model of ASD. *Nat Neurosci*. 2020;23(4):520–532.
- Colantuoni C, Lipska BK, Ye T, Hyde TM, Tao R, Leek JT, Colantuoni EA, Elkahoul AG, Herman MM, Weinberger DR, et al. Temporal dynamics and genetic control of transcription in the human prefrontal cortex. *Nature*. 2011;478(7370):519–523.
- Custo Greig L, Woodworth M, Galazo M, Padmanabhan H, Macklis J. Molecular logic of neocortical projection neuron specification, development and diversity. *Nat Rev Neurosci*. 2013;14(11):755–769.
- Dong H-M, Margulies DS, Zuo X-N, Holmes AJ. Shifting gradients of macroscale cortical organization mark the transition from childhood to adolescence. *Proc Natl Acad Sci U S A*. 2021;118(28):e2024448118–e2024448127.
- Dong D, Yao D, Wang Y, Hong S-J, Genon S, Xin F, Jung K, He H, Chang X, Duan M, et al. Compressed sensorimotor-to-transmodal hierarchical organization in schizophrenia. *Psychol Med*. 2021;8:1–14.
- Dosenbach NUF, Nardos B, Cohen AL, Fair DA, Power JD, Church JA, Nelson SM, Wig GS, Vogel AC, Lessov-Schlaggar CN, et al. Prediction of individual brain maturity using fMRI. *Science*. 2010;329(5997):1358–1361.
- Faust TE, Gunner G, Schafer DP. Mechanisms governing activity-dependent synaptic pruning in the developing mammalian CNS. *Nat Rev Neurosci*. 2021;22(11):657–673.
- Fonov V, Evans AC, Botteron K, Almli CR, McKinsty RC, Collins DL. Unbiased average age-appropriate atlases for pediatric studies. *NeuroImage*. 2011;54(1):313–327.
- Frome RC. Plasticity of cortical excitatory-inhibitory balance. *Annu Rev Neurosci*. 2015;38(1):195–219.
- Gao W, Zhu H, Giovanello KS, Smith JK, Shen D, Gilmore JH, Lin W. Evidence on the emergence of the brain's default network from 2-week-old to 2-year-old healthy pediatric subjects. *Proc Natl Acad Sci U S A*. 2009;106(16):6790–6795.
- Gao W, Alcauter S, Elton A, Hernandez-Castillo CR, Smith JK, Ramirez J, Lin W. Functional network development during the first year: relative sequence and socioeconomic correlations. *Cereb Cortex*. 2015;25(9):2919–2928.
- Gao W, Alcauter S, Smith JK, Gilmore JH, Lin W. Development of human brain cortical network architecture during infancy. *Brain Struct Funct*. 2015;220(2):1173–1186.
- Glahn DC, Winkler AM, Kochunov P, Almasy L, Duggirala R, Carless MA, Curran JC, Olvera RL, Laird AR, Smith SM, et al. Genetic control over the resting brain. *Proc Natl Acad Sci U S A*. 2010;107(3):1223–1228.
- Glasser MF, Sotiropoulos SN, Wilson JA, Coalson TS, Fischl B, Andersson JL, Xu J, Jbabdi S, Webster M, Polimeni JR, et al. The minimal preprocessing pipelines for the Human Connectome Project. *NeuroImage*. Mapping the Connectome. 2013;80:105–124.
- Golumbeanu M. TMixClust: time series clustering of gene expression with gaussian mixed-effects models and smoothing splines. 2021.
- Grothe MJ, Sepulcre J, Gonzalez-Escamilla G, Jelicstratova I, Schöll M, Hansson O, Teipel SJ, Alzheimer's Disease Neuroimaging Initiative. Molecular properties underlying regional vulnerability to Alzheimer's disease pathology. *Brain*. 2018;141(9):2755–2771.
- Gu S, Satterthwaite TD, Medaglia JD, Yang M, Gur RE, Gur RC, Bassett DS. Emergence of system roles in normative neurodevelopment. *Proc Natl Acad Sci U S A*. 2015;112(44):13681–13686.
- Hagmann P, Sporns O, Madan N, Cammoun L, Pienaar R, Wedeen VJ, Meuli R, Thiran J-P, Grant PE. White matter maturation reshapes structural connectivity in the late developing human brain. *Proc Natl Acad Sci U S A*. 2010;107(44):19067–19072.
- Hansen JY, Markello RD, Vogel JW, Seidlitz J, Bzdok D, Misic B. Mapping gene transcription and neurocognition across human neocortex. *Nat Hum Behav*. 2021;5(9):1240–1250.

- Harms MP, Somerville LH, Ances BM, Andersson J, Barch DM, Bastiani M, Bookheimer SY, Brown TB, Buckner RL, Burgess GC, et al. Extending the Human Connectome Project across ages: imaging protocols for the lifespan development and aging projects. *NeuroImage*. 2018;183:972–984.
- Hawrylycz MJ, Lein ES, Guillozet-Bongaarts AL, Shen EH, Ng L, Miller JA, van de Lagemaat LN, Smith KA, Ebbert A, Riley ZL, et al. An anatomically comprehensive atlas of the adult human brain transcriptome. *Nature*. 2012;489(7416):391–399.
- van den Heuvel MP, Kersbergen KJ, de Reus MA, Keunen K, Kahn RS, Groenendaal F, de Vries LS, Benders MJNL. The neonatal connectome during preterm brain development. *Cereb Cortex*. 2015;25(9):3000–3013.
- Hill J, Inder T, Neil J, Dierker D, Harwell J, Essen DV. Similar patterns of cortical expansion during human development and evolution. *Proc Natl Acad Sci U S A*. 2010;107(29):13135–13140.
- Hodge MR, Horton W, Brown T, Herrick R, Olsen T, Hileman ME, McKay M, Archie KA, Cler E, Harms MP, et al. ConnectomeDB—sharing human brain connectivity data. *NeuroImage*. 2016;124(Pt B):1102–1107.
- Hodge RD, Bakken TE, Miller JA, Smith KA, Barkan ER, Graybuck LT, Close JL, Long B, Johansen N, Penn O. Conserved cell types with divergent features in human versus mouse cortex. *Nature*. 2019;573(7772):61–68.
- Hong S-J, Vos de Wael R, Bethlehem RAI, Larivière S, Paquola C, Valk SL, Milham MP, Di Martino A, Margulies DS, Smallwood J, et al. Atypical functional connectome hierarchy in autism. *Nat Commun*. 2019;10(1):1022–1034.
- Hubert L, Arabie P. Comparing partitions. *J Classif*. 1985;2(1):193–218.
- Huntenburg JM, Bazin P-L, Margulies DS. Large-scale gradients in human cortical organization. *Trends Cogn Sci*. 2018;22(1):21–31.
- Kang HJ, Kawasawa YI, Cheng F, Zhu Y, Xu X, Li M, Sousa AMM, Pletikos M, Meyer KA, Sedmak G, et al. Spatio-temporal transcriptome of the human brain. *Nature*. 2011;478(7370):483–489.
- King KM, Littlefield AK, McCabe CJ, Mills KL, Flournoy J, Chassin L. Longitudinal modeling in developmental neuroimaging research: common challenges, and solutions from developmental psychology. *Dev Cogn Neurosci*. Methodological Challenges in Developmental Neuroimaging: Contemporary Approaches and Solutions. 2018;33:54–72.
- Korotkevich G, Sukhov V, Budin N, Shpak B, Artyomov MN, Sergushichev A. Fast gene set enrichment analysis. 2021.
- Kozol R. Prenatal neuropathologies in autism spectrum disorder and intellectual disability: the gestation of a comprehensive Zebrafish model. *JDB*. 2018;6(4):29–55.
- Lake BB, Chen S, Sos BC, Fan J, Kaeser GE, Yung YC, Duong TE, Gao D, Chun J, Kharchenko PV, et al. Integrative single-cell analysis of transcriptional and epigenetic states in the human adult brain. *Nat Biotechnol*. 2018;36(1):70–80.
- Langs G, Golland P, Ghosh SS. Predicting activation across individuals with resting-state functional connectivity based multi-atlas label fusion. In: Navab N, Hornegger J, Wells WM, Frangi A, editors. *Medical image computing and computer-assisted intervention—MICCAI 2015. Lecture notes in computer science*. Cham: Springer International Publishing; 2015. pp. 313–320.
- Larivière S, Vos de Wael R, Hong S-J, Paquola C, Tavakol S, Lowe AJ, Schrader DV, Bernhardt BC. Multiscale structure–function gradients in the neonatal connectome. *Cereb Cortex*. 2020;30(1):47–58.
- Larsen B, Cui Z, Adebimpe A, Pines A, Alexander-Bloch A, Bertolero M, Calkins ME, Gur RE, Gur RC, Mahadevan AS, et al. A developmental reduction of the excitation:inhibition ratio in association cortex during adolescence. *Sci Adv*. 2022;8(5):eabj8750–eabj8761.
- Lavin A, Moore HM, Grace AA. Prenatal disruption of neocortical development alters prefrontal cortical neuron responses to dopamine in adult rats. *Neuropsychopharmacology*. 2005;30(8):1426–1435.
- Li G, Lin W, Gilmore JH, Shen D. Spatial patterns, longitudinal development, and hemispheric asymmetries of cortical thickness in infants from birth to 2 years of age. *J Neurosci*. 2015;35(24):9150–9162.
- Lodge DJ, Grace AA. Gestational methylazoxymethanol acetate administration: a developmental disruption model of schizophrenia. *Behav Brain Res*. 2009;204(2):306–312.
- Marcus DS, Harms MP, Snyder AZ, Jenkinson M, Wilson JA, Glasser MF, Barch DM, Archie KA, Burgess GC, Ramaratnam M, et al. Human connectome project informatics: quality control, database services, and data visualization. *NeuroImage*. Mapping the Connectome. 2013;80:202–219.
- Margulies DS, Ghosh SS, Goulas A, Falkiewicz M, Huntenburg JM, Langs G, Bezgin G, Eickhoff SB, Castellanos FX, Petrides M, et al. Situating the default-mode network along a principal gradient of macroscale cortical organization. *Proc Natl Acad Sci U S A*. 2016;113(44):12574–12579.
- Markello RD, Arnatkeviciute A, Poline J-B, Fulcher BD, Fornito A, Misis B. Standardizing workflows in imaging transcriptomics with the abagen toolbox. *elife*. 2021;10:e72129–e72156.
- Markicevic M, Fulcher BD, Lewis C, Helmchen F, Rudin M, Zerbi V, Wenderoth N. Cortical excitation:inhibition imbalance causes abnormal brain network dynamics as observed in neurodevelopmental disorders. *Cereb Cortex*. 2020;30(9):4922–4937.
- Martins D, Giacometti A, Williams SCR, Turkheimer F, Dipasquale O, Veronese M. Imaging transcriptomics: convergent cellular, transcriptomic, and molecular neuroimaging signatures in the healthy adult human brain. *Cell Rep*. 2021;37(13):110173–110190.
- Mesulam M. The evolving landscape of human cortical connectivity: facts and inferences. *NeuroImage*. 2012;62(4):2182–2189.
- Metcalf WK, Myers PZ, Trevarrow B, Bass MB, Kimmel CB. Primary neurons that express the L2/HNK-1 carbohydrate during early development in the zebrafish. *Development*. 1990;110(2):491–504.
- Morgan SE, Seidlitz J, Whitaker KJ, Romero-Garcia R, Clifton NE, Scarpazza C, van Amelsvoort T, Marcelis M, van Os J, Donohoe G, et al. Cortical patterning of abnormal morphometric similarity in psychosis is associated with brain expression of schizophrenia-related genes. *Proc Natl Acad Sci U S A*. 2019;116(19):9604–9609.
- Murphy C, Jefferies E, Rueschemeyer S-A, Sormaz M, Wang H-T, Margulies DS, Smallwood J. Distant from input: evidence of regions within the default mode network supporting perceptually-decoupled and conceptually-guided cognition. *NeuroImage*. 2018;171:393–401.
- Nenning K-H, Xu T, Schwartz E, Arroyo J, Woehrer A, Franco AR, Vogelstein JT, Margulies DS, Liu H, Smallwood J, et al. Joint embedding: a scalable alignment to compare individuals in a connectivity space. *NeuroImage*. 2020;222:117232–117243.
- O'Donnell KJ, Meaney MJ. Fetal origins of mental health: the developmental origins of health and disease hypothesis. *AJP*. 2017;174(4):319–328.
- Ortiz-Terán L, Diez I, Ortiz T, Perez DL, Aragón JI, Costumero V, Pascual-Leone A, El Fakhri G, Sepulcre J. Brain circuit–gene expression relationships and neuroplasticity of multisensory cortices in blind children. *Proc Natl Acad Sci U S A*. 2017;114(26):6830–6835.
- Parenti I, Rabaneda LG, Schoen H, Novarino G. Neurodevelopmental disorders: from genetics to functional pathways. *Trends Neurosci*. 2020;43(8):608–621.

- Patel Y, Writing Committee for the Attention-Deficit/Hyperactivity Disorder, Autism Spectrum Disorder, Bipolar Disorder, Major Depressive Disorder, Obsessive-Compulsive Disorder, and Schizophrenia ENIGMA Working Groups. Virtual histology of cortical thickness and shared neurobiology in 6 psychiatric disorders. *JAMA Psychiat*. 2021;78(1):47–63.
- Piñero J, Ramírez-Angueta JM, Saüch-Pitarch J, Ronzano F, Centeno E, Sanz F, Furlong LI. The DisGeNET knowledge platform for disease genomics: 2019 update. *Nucleic Acids Res*. 2020;48(D1):D845–D855.
- Poldrack R, Kittur A, Kalar D, Miller E, Seppa C, Gil Y, Parker D, Sabb F, Bilder R. The cognitive atlas: toward a knowledge foundation for cognitive neuroscience. *Front Neuroinform*. 2011;5:17–27.
- Raut RV, Snyder AZ, Raichle ME. Hierarchical dynamics as a macroscopic organizing principle of the human brain. *PNAS*. 2020;117(34):20890–20897.
- Reineberg AE, Hatoum AS, Hewitt JK, Banich MT, Friedman NP. Genetic and environmental influence on the human functional connectome. *Cereb Cortex*. 2020;30(4):2099–2113.
- Reynolds JE, Long X, Paniukov D, Bagshawe M, Lebel C. Calgary Preschool magnetic resonance imaging (MRI) dataset. *Data Brief*. 2020;29:105224–105229.
- Richiardi J, Altmann A, Milazzo A-C, Chang C, Chakravarty MM, Banaschewski T, Barker GJ, Bokde ALW, Bromberg U, Büchel C, et al. Correlated gene expression supports synchronous activity in brain networks. *Science*. 2015;348(6240):1241–1244.
- Romero-Garcia R, Warrier V, Bullmore ET, Baron-Cohen S, Bethlehem RAL. Synaptic and transcriptionally downregulated genes are associated with cortical thickness differences in autism. *Mol Psychiatry*. 2019;24(7):1053–1064.
- Rousseeuw PJ. Silhouettes: a graphical aid to the interpretation and validation of cluster analysis. *J Comput Appl Math*. 1987;20:53–65.
- Rubenstein JLR, Merzenich MM. Model of autism: increased ratio of excitation/inhibition in key neural systems. *Genes Brain Behav*. 2003;2(5):255–267.
- Sakai J. Core concept: how synaptic pruning shapes neural wiring during development and, possibly, in disease. *Proc Natl Acad Sci U S A*. 2020;117(28):16096–16099.
- Salimi-Khorshidi G, Douaud G, Beckmann CF, Glasser MF, Griffanti L, Smith SM. Automatic denoising of functional MRI data: combining independent component analysis and hierarchical fusion of classifiers. *NeuroImage*. 2014;90:449–468.
- Satterthwaite TD, Elliott MA, Ruparel K, Loughhead J, Prabhakaran K, Calkins ME, Hopson R, Jackson C, Keefe J, Riley M, et al. Neuroimaging of the Philadelphia neurodevelopmental cohort. *NeuroImage*. 2014;86:544–553.
- Schaefer A, Kong R, Gordon EM, Laumann TO, Zuo X-N, Holmes AJ, Eickhoff SB, Yeo BTT. Local-global parcellation of the human cerebral cortex from intrinsic functional connectivity MRI. *Cereb Cortex*. 2018;28(9):3095–3114.
- Seabold S, Perktold J. 2010. Statsmodels: econometric and statistical modeling with Python. Presented at the Python in Science Conference. Austin, Texas. p. 92–96.
- Shafiei G, Markello RD, Vos de Wael R, Bernhardt BC, Fulcher BD, Misic B. Topographic gradients of intrinsic dynamics across neocortex. *elife*. 2020;9:e62116–e62137.
- Silbereis JC, Pochareddy S, Zhu Y, Li M, Sestan N. The cellular and molecular landscapes of the developing human central nervous system. *Neuron*. 2016;89(2):248–268.
- Sohal VS, Rubenstein JLR. Excitation-inhibition balance as a framework for investigating mechanisms in neuropsychiatric disorders. *Mol Psychiatry*. 2019;24(9):1248–1257.
- Solinas M, Chauvet C, Thiriet N, El Rawas R, Jaber M. Reversal of cocaine addiction by environmental enrichment. *Proc Natl Acad Sci U S A*. 2008;105(44):17145–17150.
- Stuart T, Butler A, Hoffman P, Hafemeister C, Papalexi E, Mauck WM, Hao Y, Stoeckius M, Smibert P, Satija R. Comprehensive integration of single-cell data. *Cell*. 2019;177(7):1888–1902.
- Subramanian L, Calcagnotto ME, Paredes MF. Cortical malformations: lessons in human brain development. *Front Cell Neurosci*. 2020;13:576.
- Sydner VJ, Larsen B, Bassett DS, Alexander-Bloch A, Fair DA, Liston C, Mackey AP, Milham MP, Pines A, Roalf DR, et al. Neurodevelopment of the association cortices: patterns, mechanisms, and implications for psychopathology. *Neuron*. 2021;18(18):2820–2846.
- Thomas MJ, Beurrier C, Bonci A, Malenka RC. Long-term depression in the nucleus accumbens: a neural correlate of behavioral sensitization to cocaine. *Nat Neurosci*. 2001;4(12):1217–1223.
- Tierney AL, Nelson CA. Brain development and the role of experience in the early years. *Zero Three*. 2009;30(2):9–13.
- Vos de Wael R, Benkarim O, Paquola C, Larivière S, Royer J, Tavakol S, Xu T, Hong S-J, Langs G, Valk S, et al. BrainSpace: a toolbox for the analysis of macroscale gradients in neuroimaging and connectomics datasets. *Commun Biol*. 2020;3(1):1–10.
- Whitaker KJ, Vértes PE, Romero-Garcia R, Váša F, Moutoussis M, Prabhu G, Weiskopf N, Callaghan MF, Wagstyl K, Rittman T, et al. Adolescence is associated with genomically patterned consolidation of the hubs of the human brain connectome. *Proc Natl Acad Sci U S A*. 2016;113(32):9105–9110.
- Winder DG, Egli RE, Schramm NL, Matthews RT. Synaptic plasticity in drug reward circuitry. *Curr Mol Med*. 2002;2(7):667–676.
- Wu T, Hu E, Xu S, Chen M, Guo P, Dai Z, Feng T, Zhou L, Tang W, Zhan L, et al. clusterProfiler 4.0: a universal enrichment tool for interpreting omics data. *Innovation*. 2021;2(3):100141–100151.
- Xia Y, Xia M, Liu J, Liao X, Lei T, Liang X, Zhao T, Shi Z, Sun L, Chen X, et al. Development of functional connectome gradients during childhood and adolescence. *Sci Bull*. 2022;67(10):1049–1061.
- Yarkoni T, Poldrack RA, Nichols TE, Van Essen DC, Wager TD. Large-scale automated synthesis of human functional neuroimaging data. *Nat Methods*. 2011;8(8):665–670.
- Zeng L-L, Wang D, Fox MD, Sabuncu M, Hu D, Ge M, Buckner RL, Liu H. Neurobiological basis of head motion in brain imaging. *Proc Natl Acad Sci U S A*. 2014;111(16):6058–6062.
- Zoghbi HY, Bear MF. Synaptic dysfunction in neurodevelopmental disorders associated with autism and intellectual disabilities. *Cold Spring Harb Perspect Biol*. 2012;4(3):a009886.